Single and two photon time resolved polarised fluorescence studies of probe molecule dynamics in nematic liquid crystals.

E. M. Monge, D. A. Armoogum and A. J. Bain*

Department of Physics & Astronomy, University College London, Gower Street, London WC1E 6BT, UK

ABSTRACT

We present the results of combined single and two photon linearly polarised time resolved fluorescence anisotropy measurements of the order and motion of a fluorescent probe (rhodamine 6G) in the nematic phase of 4-n-pentyl4'-cyanobiphenyl (5CB). Variation of the excitation polarisation angle (β) with respect to the nematic director yield a set of initial single and two photon anisotropies R(0,β). Single photon R(0,β) measurements yield the $<P_2>$ and $<P_4>$ moments of the ground state orientational distribution function. For rhodamine 6G in 5CB these indicate that the inclusion of higher moments ($<P_6>$ and above) are necessary to describe the probe ordering within the nematic host.. Two photon R(0,β) measurements however allow the direct measurement of $<P_6>$, for rhodamine 6G these yield a value close to theoretical predictions. Two and single photon initial anisotropy measurements are wholly consistent with an approximately Gaussian probe distribution at an angle of 38° to the nematic director with a full width half maximum of c.a. 26°. Variation of β affords the photoselection of both cylindrically symmetric and asymmetric degrees of probe alignment that are sensitive respectively to θ and θ plus ϕ diffusion in the laboratory (nematic director) frame. Cylindrically symmetric and asymmetric alignment relaxation are observed to be linear but with distinctly different relaxation rates, indicating highly restricted probe motion within the nematic environment.

Keywords: fluorescent probe, liquid crystal, order parameters, two photon, photoselection, fluorescence anisotropy, orientational relaxation, diffusion, rhodamine 6G

1. INTRODUCTION

Time resolved single photon polarised fluorescence measurements have been widely used to probe molecular dynamics and photophysics in condensed phases[1-3] together with the study of local structure and dynamics in biomolecular assemblies[4-5]. In these latter studies the fluorescent probe experiences a locally ordered molecular environment however the distribution of these environments in the laboratory frame is wholly random. As a result of this averaging process much useful information is lost. Recent work in our group has shown for an ordered medium (i.e. a non random distribution of probe environments) polarised time resolved fluorescence when coupled with a variable excitation polarisation can yield hitherto unobserved information on molecular order and dynamics[6-9]. Variation of the (linear) excitation polarisation in the laboratory frame allows the preparation of a range of non-equilibrium probe orientational distributions *within* the (ordered) local environment. The evolution of these distributions is monitored using picosecond time resolved fluorescence polarisation (see figure 1). For systems possessing cylindrical symmetry we have shown that it is possible to determine the full angular motion (θ and ϕ diffusion) together with the second $<P_2>$ and fourth order parameters $<P_4>$ of the ground state distribution function[7-9]. Recent work in our group has extended these techniques to the study of probe motion and order in nematic liquid crystals[9-12]. The ordering of fluorescent probes within liquid crystals such as 5CB is pronounced, single photon fluorescence anisotropy measurements indicate that the inclusion of additional order parameters ($<P_K>$ K>4) in the ground state distribution function are necessary. Raman scattering[13] and two photon dichroism[14] have been used to determine the second and fourth order moments of the nematic phase of pure 5CB. To date the direct determination of higher degrees of molecular order (K>4) in the nematic phase has to our knowledge not been realised.

*Corresponding author, email a.bain@ucl.ac.uk

Multiphoton Absorption and Nonlinear Transmission Processes: Materials, Theory, and Applications, K. D. Belfield, S. J. Caracci, F. Kajzar, C. M. Lawson, A. T. Yeates, Editors, Proceedings of SPIE Vol. 4797 © 2003 SPIE · 0277-786X/03/$15.00

As will be seen, the combination of variable single and two photon photoselection techniques yield not only the θ and ϕ probe diffusion rates but value of the predicted (but hitherto unobserved) sixth order parameter $\langle P_6 \rangle$ of the ground state probe distribution function.

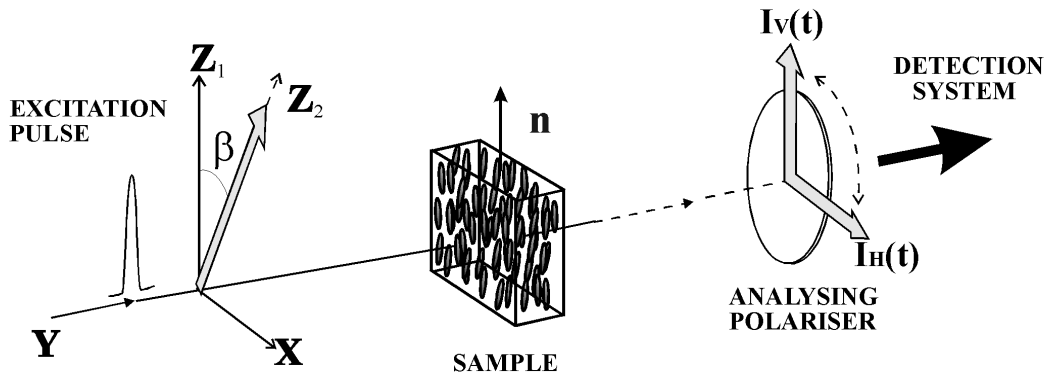

Figure 1. Schematic 180° excitation detection experimental geometry utilising a variably polarised (β) excitation pulse. Collection of the fluorescence components in the V (or Z) and H (or X) directions are used to construct the fluorescence anisotropy function R(t,β)

2. PROBE ORDER IN THE NEMATIC MESOPHASE

In a nematic mesophase molecular order is conveniently expressed in a spherical polar co-ordinate system the Z axis of which is defined by the nematic director. In such a system the probability P(θ,ϕ) of finding a probe molecule oriented between the polar angle θ and θ+dθ, and the azimuthal angles ϕ and ϕ+dϕ can be conveniently expressed in terms of an expansion in spherical harmonics

$$P(\theta,\phi) = \sum_{KQ} \langle C_{KQ} \rangle Y_{KQ}(\theta,\phi) \tag{1}$$

where the moments $\langle C_{KQ} \rangle$ or order parameters of the distribution correspond to direct physical observables. The axial and symmetry and even parity of the mesophase restricts the rank K of the moments to be even and their projection Q to be zero. An alternative formulation of the distribution function in terms of Legendre polynomials reflects this symmetry,

$$P(\theta) = \sum_{K} \langle P_K \rangle P_K(\theta) \tag{2}$$

The relation between the two order parameters being given by

$$\langle P_K \rangle = \frac{\langle C_{K0} \rangle}{\langle C_{00} \rangle \sqrt{2K+1}} = \frac{\langle \alpha_{K0} \rangle}{\sqrt{2K+1}} \tag{3}$$

where $\langle \alpha_{K0} \rangle$ is the normalised moment of the distribution function[7]. In fluorescence anisotropy experiments where cylindrical asymmetry is deliberately created in the excited state probe distribution the former distribution function is necessary to describe fully the fluorescence anisotropy and to interpret its evolution[7].

3. FLUORESCENCE ANISOTROPY .

In both two and single photon excitation single photon emission is observed from S_1 to higher vibrational levels of the S_0 ground state (figure 2). We have shown that irrespective of the excitation process the measurement of fluorescence anisotropy from an arbitrarily ordered excited state is determined solely by the cylindrically symmetric and asymmetric

degrees of molecular alignment[7]. In the co-ordinate system of figure 1 the time resolved fluorescence anisotropy is given by

$$R(t)=\frac{I_V(t)-I_H(t)}{I_V(t)+2I_H(t)}=\frac{\frac{\langle\alpha_{20}^{ex}(t)\rangle}{\sqrt{5}}-\frac{1}{\sqrt{30}}\left\{\langle\alpha_{22}^{ex}(t)\rangle+\langle\alpha_{2-2}^{ex}(t)\rangle\right\}}{1+\frac{2}{\sqrt{30}}\left\{\langle\alpha_{22}^{ex}(t)\rangle+\langle\alpha_{2-2}^{ex}(t)\rangle\right\}} \tag{4}$$

where $\langle\alpha_{20}^{ex}(t)\rangle$ and $\left\{\langle\alpha_{22}^{ex}(t)\rangle+\langle\alpha_{2-2}^{ex}(t)\rangle\right\}$ are the time dependent cylindrically symmetric and asymmetric degrees of excited state alignment. Their initial values are dependent on the photoselection process and the degree of order in the ground state. From symmetry considerations the alignment relaxation dynamics in an ordered medium with cylindrical symmetry are of the form[7,12].

$$\begin{aligned}\langle\alpha_{20}^{ex}(t)\rangle&=\left\{\langle\alpha_{20}^{ex}(0)\rangle-\langle\alpha_{20}^{ex}(ss)\rangle\right\}\exp\left(-\frac{t}{\tau_{20}}\right)+\langle\alpha_{20}^{ex}(ss)\rangle\\ \left\{\langle\alpha_{22}^{ex}(t)\rangle+\langle\alpha_{2-2}^{ex}(t)\rangle\right\}&=\left\{\langle\alpha_{22}^{ex}(0)\rangle+\langle\alpha_{2-2}^{ex}(0)\rangle\right\}\exp\left(-\frac{t}{\tau_{22}}\right)\end{aligned} \tag{5}$$

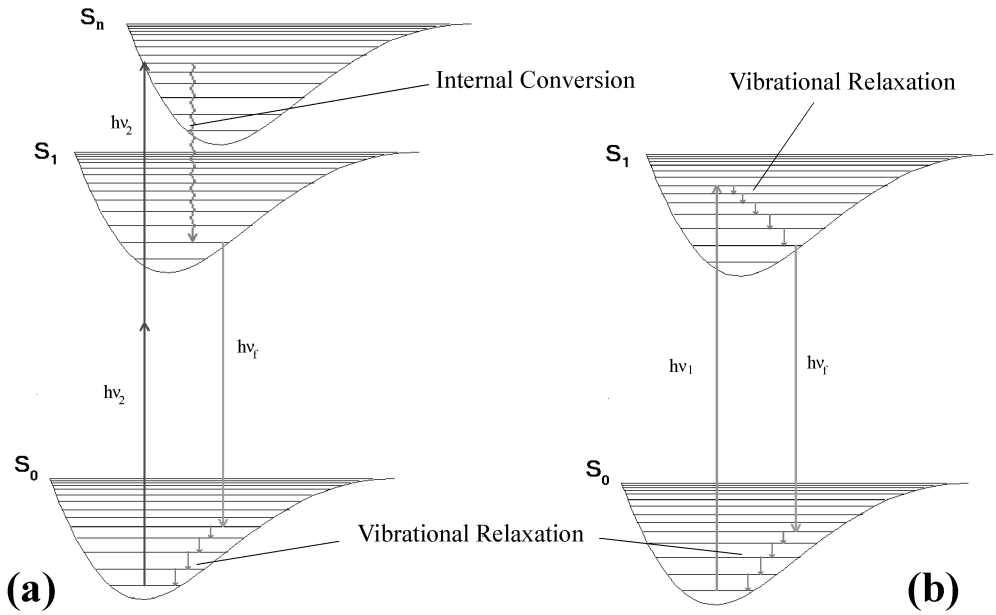

Figure 2. (a) Schematic representation of two photon excitation in a molecular probe such as rhodamine 6G, initial excitation is via the simultaneous absorption of two near infra red photons (c.a. 800nm) with rapid relaxation to vibrationally excited levels in the S_1 excited electronic state. Rapid vibrational relaxation in S_1 (sub-picosecond) is followed by fluorescence to vibrationally excited levels in the S_0 ground state. (b) In single photon excitation high lying vibrational levels in S_1 are directly accessed by absorption of a visible (575nm) photon. Rapid (sub-picosecond) vibrational relaxation is followed by emission to high lying vibrational levels in the electronic ground state.

where (ss) denotes the equilibrium or steady state value of the probe alignment. The cylindrically symmetric and asymmetric alignment rates τ_{20} and τ_{22} are related to the θ and ϕ diffusion rates in the laboratory frame $D_{\perp}^{LAB}$ and $D_{\parallel}^{LAB}$ respectively through

$$\frac{1}{\tau_{20}} = 6D_{\perp}^{LAB} \tag{6}$$

$$\frac{1}{\tau_{22}} = 2D_{\perp}^{LAB} + 4D_{\parallel}^{LAB} \tag{7}$$

The fluorescence anisotropy is thus strongly dependent on the degree of ground state order, the nature of the photoselection process and the excited state dynamics. From the initial value of the fluorescence anisotropy (i.e. prior to the onset of orientational relaxation) it is possible, given knowledge of the angular dependence of the excitation process to determine moments of the round state probe distribution function.

4 SINGLE AND TWO PHOTON PHOTOSELECTION

For single photon excitation variation of the excitation polarisation angle β in the laboratory frame is leads to a transition probability of the form[7]

$$W_{SP}(\theta,\phi,t) = B\frac{\sqrt{4\pi}}{3}\left[\quad Y_{00}(\theta,\phi) + \frac{2}{\sqrt{5}}\sum_{q} d^{2}_{q0}(-\beta)Y_{2q}(\theta,\phi)\right] \tag{8}$$

where B is a constant of proportionality. and $d^{2}_{q0}(-\beta)$ is a reduced rotation matrix[19]. Setting β=0° the conventional $\cos^2\theta$ transition probability is recovered. For two photon excitation the transition probability is more sharply peaked (exhibiting a $\cos^4\theta$ dependence), the equivalent relation to (8) is given by[3]

$$W_{TP}(\theta,\phi) = B'\frac{\sqrt{4\pi}}{5}\left[Y_{00}(\theta,\phi) + \frac{20}{7\sqrt{5}}\sum_{q} d^{2}_{q0}(-\beta)Y_{2q0}(\theta,\phi) + \frac{8}{21}\sum_{q} d^{4}_{q0}(-\beta)Y_{4q}(\theta,\phi)\right] \tag{9}$$

where B′ is a constant depending on the laser pulse energy width and degree of coherence and two photon absorption cross section. Assuming that either excitation process is weak (i.e. no optical pumping of the probe ground state) the initial excited state distribution function can be expressed as the product of the transition probability and the ground state distribution function. The initial moments of the excited state distribution are given by[7]

$$\left\langle C^{ex}_{KQ}(0)\right\rangle = \int_{0}^{2\pi}\int_{0}^{\pi} Y^{*}_{KQ}(\theta,\phi)W(\theta,\phi)P_{gs}(\theta,\phi)\sin\theta d\theta d\phi \tag{10}$$

Expansion of the ground state distribution as in (2) and insertion of (8) and (9) into (10) the single and two photon excited state moments are respectively,

$$\left\langle C^{ex}_{KQ}(0,sp)\right\rangle = B\frac{\sqrt{4\pi}}{3}\sum_{K'}\left\langle C^{gs}_{K'0}(ss)\right\rangle\left\langle KQ\right|\left[\quad Y_{00}(\theta,\phi) + \frac{2}{\sqrt{5}}\sum_{q} d^{2}_{q0}(-\beta)Y_{2q}(\theta,\phi)\right]\left|K'0\right\rangle \tag{11}$$

$$\left\langle C^{ex}_{KQ}(0,tp)\right\rangle = B'\frac{\sqrt{4\pi}}{5}\sum_{K'}\left\langle C^{gs}_{K'0}(ss)\right\rangle\left\langle KQ\right|\begin{bmatrix} Y_{00}(\theta,\phi) + \frac{20}{7\sqrt{5}}\sum_{q} d^{2}_{q0}(-\beta)Y_{2q}(\theta,\phi) \\ + \frac{8}{21}\sum_{q} d^{4}_{q0}(-\beta)Y_{4q}(\theta,\phi)\end{bmatrix}\left|K'0\right\rangle \tag{12}$$

Two-photon excitation results in the creation of more highly polarised arrays than in the case of single photon excitation[16], this can be seen from figure 3 which compares the degrees of initial alignment that can be prepared by single and two photon excitation from an isotropic ground state. The advantage of combining two and single photon

excitation is twofold, firstly the interaction between the radiation and the polarised molecular array now allows the direct contribution of higher ground state moments through then $Y_{4q}(\theta\phi)$ term in equation (9) to the initial fluorescence anisotropy[14,17,18], thus allowing a more accurate picture of the initial molecular order to be obtained.

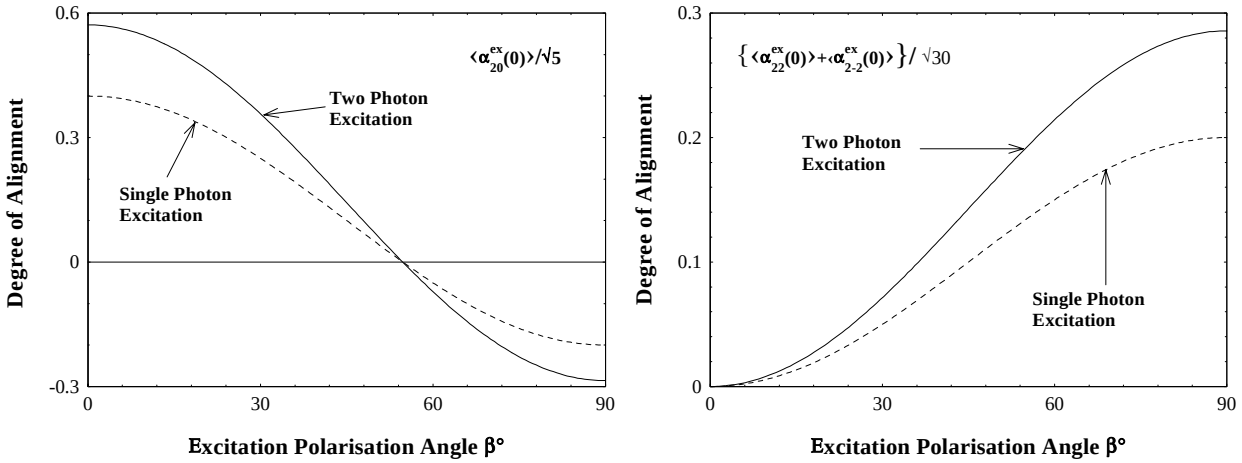

Figure 3. Variation in the initial degrees of cylindrically symmetric and asymmetric alignment produced in single and two photon excitation from an isotropic medium

Evaluating matrix[19] elements in (11) and (12) yields

$$\left\langle C_{KQ}^{ex}(0,sp)\right\rangle = \frac{B}{3}\sum_{K'q}\left\langle C_{K'0}^{gs}(ss)\right\rangle\left[\delta_{K'K}\delta_{Q0} + \frac{2}{\sqrt{5}}d_q^2(-\beta)\begin{pmatrix} K & 2 & K' \\ -Q & q & 0\end{pmatrix}\begin{pmatrix} K & 2 & K' \\ 0 & 0 & 0\end{pmatrix}\sqrt{5}\hat{K}\hat{K}'\right] \tag{13}$$

$$\left\langle C_{KQ}^{ex}(0,tp)\right\rangle = \frac{B'}{5}\sum_{K'}\left\langle C_{K'0}^{gs}(ss)\right\rangle\left[\begin{array}{l}\delta_{KK'}\delta_{Q0} + \frac{20}{7}\sum_q d_{0q}^2(-\beta)\begin{pmatrix} K & 2 & K' \\ -Q & q & 0\end{pmatrix}\begin{pmatrix} K & 2 & K' \\ 0 & 0 & 0\end{pmatrix}\hat{K}\hat{K}'\delta_{Qq} \\ + \frac{8}{7}\sum_q d_{0q}^4(-\beta)\begin{pmatrix} K & 4 & K' \\ -Q & q & 0\end{pmatrix}\begin{pmatrix} K & 4 & K' \\ 0 & 0 & 0\end{pmatrix}\hat{K}\hat{K}'\delta_{Qq}\end{array}\right] \tag{14}$$

The initial fluorescence observables are given by

$$\left\langle \alpha_{20}^{ex}(0,sp)\right\rangle = \frac{\sum_{K'q}\left\langle C_{K'0}^{gs}(ss)\right\rangle\left[\delta_{K'2} + \frac{2}{\sqrt{5}}d_{0-q}^2(-\beta)\begin{pmatrix} 2 & 2 & K' \\ 0 & 0 & 0\end{pmatrix}^2\sqrt{5}\hat{K}\hat{K}'\right]}{\sum_{K'q}\left\langle C_{K'0}^{gs}(ss)\right\rangle\left[\delta_{K'0} + \frac{2}{\sqrt{5}}d_{0-q}^2(-\beta)\delta_{K'2} + \right]} \tag{15}$$

$$\left\langle \alpha_{2\pm2}^{ex}(0,sp)\right\rangle = \frac{\sum_{K'q}\left\langle C_{K'0}^{gs}(ss)\right\rangle\left[\frac{2}{\sqrt{5}}d_{0-q}^2(-\beta)\begin{pmatrix} 2 & 2 & K' \\ \mp 2 & q & 0\end{pmatrix}\begin{pmatrix} 2 & 2 & K' \\ 0 & 0 & 0\end{pmatrix}\sqrt{5}\hat{K}\hat{K}'\right]}{\sum_{K'q}\left\langle C_{K'0}^{gs}(ss)\right\rangle\left[\delta_{K'0} + \frac{2}{\sqrt{5}}d_{00}^2(-\beta)\delta_{K'2}\right]} \tag{16}$$

$$\left\langle \alpha_{20}^{ex}(0,tp)\right\rangle = \frac{\sum_{K'}\left\langle C_{K'0}^{gs}(ss)\right\rangle\left[\delta_{KK'}\delta_{Q0}+\frac{20\sqrt{5}\hat{K}'}{7}d_{00}^{2}(-\beta)\begin{pmatrix}2&2&K'\\0&0&0\end{pmatrix}^{2}+\frac{8\sqrt{5}\hat{K}'}{7}d_{00}^{4}(-\beta)\begin{pmatrix}2&4&K'\\0&0&0\end{pmatrix}^{2}\right]}{\sum_{K'}\left\langle C_{K'0}^{gs}(ss)\right\rangle\left[\delta_{KK'}\delta_{Q0}+\frac{20}{7\sqrt{5}}d_{00}^{2}(-\beta)\delta_{K'2}+\frac{8}{21}d_{00}^{4}(-\beta)\delta_{K'4}\right]} \tag{17}$$

$$\left\langle \alpha_{2\pm2}^{ex}(0,tp)\right\rangle = \frac{\sum_{K'}\left\langle C_{K'0}^{gs}(ss)\right\rangle\left[\begin{array}{l}\frac{20\sqrt{5}\hat{K}'}{7}d_{0\pm2}^{2}(-\beta)\begin{pmatrix}2&2&K'\\\mp2&\pm2&0\end{pmatrix}\begin{pmatrix}2&2&K'\\0&0&0\end{pmatrix}\\+\frac{8\sqrt{5}\hat{K}'}{7}d_{0\pm2}^{4}(-\beta)\begin{pmatrix}2&4&K'\\\mp2&\pm2&0\end{pmatrix}\begin{pmatrix}2&4&K'\\0&0&0\end{pmatrix}\end{array}\right]}{\sum_{K'}\left\langle C_{K'0}^{gs}(ss)\right\rangle\left[\delta_{KK'}\delta_{Q0}+\frac{20}{7\sqrt{5}}d_{00}^{2}(-\beta)\delta_{K'2}+\frac{8}{21}d_{00}^{4}(-\beta)\delta_{K'4}\right]} \tag{18}$$

Insertion of (15) and (16) or (17) and (18) into (4) yields respectively, the initial single and two photon fluorescence anisotropy in terms of the ground state order parameters and the excitation polarisation angle β. From the symmetry constraints of the 3j symbols[20] it can be seen that only the K′=2 and 4 ground state order parameters can contribute to the single photon fluorescence anisotropy whereas in two photon excitation the quadrupolar term ($Y_{4q}(\theta\phi)$) in the transition probability allows the direct contribution of K′=2, 4 and 6.

Measurement of the initial single photon fluorescence anisotropy for excitation polarised parallel (β=0°) and perpendicular to the nematic director (β=90°) can thus be used to determine the K′=2 and 4 ground state order parameters. With this knowledge, measurement of the corresponding two photon initial anisotropy values permits the determination of K′= 6.

From (4) and (5) the fluorescence anisotropy should evolve according to

$$R(t) = \frac{\frac{1}{\sqrt{5}}\left[\left(\left\langle \alpha_{20}^{ex}(0)\right\rangle - \left\langle \alpha_{20}^{ex}(ss)\right\rangle\right)\exp(-t/\tau_{20}) + \left\langle \alpha_{20}^{ex}(ss)\right\rangle\right] - \frac{1}{\sqrt{30}}\left\{\left\langle \alpha_{22}^{ex}(0)\right\rangle + \left\langle \alpha_{2-2}^{ex}(0)\right\rangle\right\}\exp(-t/\tau_{22})}{1+\frac{2}{\sqrt{30}}\left\{\left\langle \alpha_{22}^{ex}(0)\right\rangle + \left\langle \alpha_{2-2}^{ex}(0)\right\rangle\right\}\exp(-t/\tau_{22})} \tag{19}$$

however in a birefringent medium the vertical and horizontally polarised components of the fluorescence anisotropy are unequally affected by local field effects and differential reflection losses at the boundary between the sample and the cell wall[14]. Application of these considerations to emission from a molecular probe in a nematic host we obtain[12] the anisotropy correction factor k given by,

$$k(\lambda,T) = \left(\frac{n_e}{n_o}\right)\left(\frac{n_o+n_g}{n_e+n_g}\right)^{2}\left(\frac{n_e^2+2}{n_o^2+2}\right) \tag{20}$$

In this analysis k is uniquely determined by the extraordinary and ordinary indices of refraction n_e and n_o respectively and the refractive index of the sample cell wall n_g. The temperature and wavelength dependence of these for 5CB are well known[21], however correction for the change in the nematic isotropic phase transition and averaging over the fluorescence emission spectrum is necessary[22]. We have recently shown that it is possible to determine k independently by a series of fluorescence lifetime and anisotropy measurements[10-11], the values yielded by both methods are in general agreement. For rhodamine 6G in 5CB at T=22.5°C k=1.130. The second correction factor the A parameter takes into account the reduction in the fluorescence anisotropy from theoretical values due the possible contribution of a number

of molecular and experimental factors. Principally these are the non-parallelism of absorption and emission transition dipole moments[7], depolarisation due arising from sample concentration and path length effects[16] and depolarisation by the collection optics. The A parameter is determined by the departure of the initial fluorescence anisotropy from its theoretical value in an isotropic sample[8]. For liquid crystalline media the sample is raised to the a few degrees above the nematic isotropic phase transition temperature where departure of R(0,β) from theory is then determined[22]. For rhodamine 6G in 5CB this approach yielded a value for A of 0.901. Finite values of k and A alter the relative contributions of the vertical and horizontally polarised fluorescence signals used to construct R(t) and to a reduction in the relative degrees of observed molecular alignment. The altered (observed) anisotropy (equation 4) becomes[10]

$$R(t)=\frac{\frac{k-1}{A}+\frac{\langle\alpha_{20}^{ex}(t)\rangle}{\sqrt{5}}(2k+1)-\sqrt{\frac{3}{10}}\left\{\langle\alpha_{22}^{ex}(t)\rangle+\langle\alpha_{2-2}^{ex}(t)\rangle\right\}}{\frac{k+2}{A}+\frac{\langle\alpha_{20}^{ex}(t)\rangle}{\sqrt{5}}(2k-2)+2\sqrt{\frac{3}{10}}\left\{\langle\alpha_{22}^{ex}(t)\rangle+\langle\alpha_{2-2}^{ex}(t)\rangle\right\}} \tag{21}$$

The time dependent fluorescence anisotropy becomes

$$R(t)=\frac{\frac{k-1}{A}+\frac{(2k+1)}{\sqrt{5}}\left[\begin{array}{l}\left[\langle\alpha_{20}^{ex}(0)\rangle-\langle\alpha_{20}^{ex}(ss)\rangle\right]\exp(-t/\tau_{20})\\+\langle\alpha_{20}^{ex}(ss)\rangle\end{array}\right]-\frac{1}{\sqrt{30}}\left\{\langle\alpha_{22}^{ex}(0)\rangle+\langle\alpha_{2-2}^{ex}(0)\rangle\right\}\exp(-t/\tau_{22})}{\frac{k+2}{A}+\frac{(2k-2)}{\sqrt{5}}\left[\begin{array}{l}\left[\langle\alpha_{20}^{ex}(0)\rangle-\langle\alpha_{20}^{ex}(ss)\rangle\right]\exp(-t/\tau_{20})\\+\langle\alpha_{20}^{ex}(ss)\rangle\end{array}\right]+\frac{2}{\sqrt{30}}\left\{\langle\alpha_{22}^{ex}(0)\rangle+\langle\alpha_{2-2}^{ex}(0)\rangle\right\}\exp(-t/\tau_{22})} \tag{22}$$

In spite of the apparent complexity of (22), the primary influence of k and A is in the determination of the static order parameters. Typical values for k in strongly ordered nematic environments are of the order of 1.1, the difference between corrected and uncorrected lifetimes is small (c.a. 10% for k=1.2)[10].

4. SINGLE AND TWO PHOTON FLUORESCENCE ANISOTROPY MEASUREMENTS.

The time correlated single photon counting system used in these studies has been described in detail elsewhere[8, 22]. Single photon excitation of rhodamine 6G at 575nm was undertaken using the 7ps output of a cavity dumped rhodamine 6G dye laser (Coherent 700) synchronously pumped by a frequency doubled Nd: YAG oscillator (Coherent Antares 76-S). Two photon excitation measurements at 800nm were performed using a portion of the 250KHz 200 fs output of a Ti:Sapphire regenerative amplifier (Coherent REGA 9000) seeded by a modelocked Ti:Sapphire oscillator (Coherent MIRA 900F). Single and two photon excited fluorescence anisotropy decays for rhodamine 6G in an isotropic medium yielded identical (to within experimental error) single exponential orientational relaxation times together with initial fluorescence anisotropies close to their theoretical values. These are shown in figure 4.

The rhodamine 6G doped nematic 5CB (c.a. 10^{-4}M) was held in 100μm thick quartz cells. To provide a homogeneous alignment for the liquid crystal environment, the cells were coated with a surfactant (polyvinyl alcohol solution) and rubbed mechanically. The cell path length of 100μm falls within the 300μm range over which homogeneous alignment persists[12].

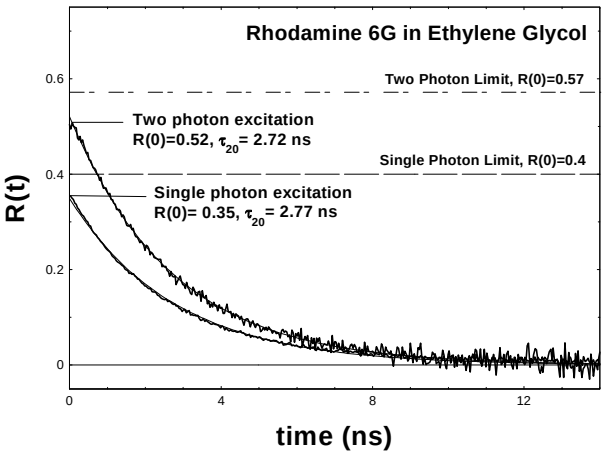

Figure 4: Single and two photon excited fluorescence anisotropy decays for rhodamine 6G in ethylene glycol, linear relaxation to an isotropic steady state is seen to take place with a characteristic alignment time of c.a. 2.7-2.8 ns is observed for both excitation schemes. The initial single and two photon fluorescence anisotropies are close to the theoretical limits for excitation from an unpolarised ground state.

5. RESULTS

Single and two photon fluorescence anisotropy decays for $\beta=0°$ and $90°$ are shown in figure 5. Irrespective of the excitation process the (corrected) fluorescence anisotropy was observed to yield steady state probe alignment of c.a. 0.3. In spite of the high degree of probe alignment the initial $\beta=0°$ fluorescence anisotropy for both excitation processes is not significantly displaced from the value obtained for excitation in an isotropic medium (see figure 4). This is due to the presence of a substantial negative $K'=4$ component of the ground state probe distribution (i.e. $\langle P_4 \rangle$). Analysis of the corrected initial single photon fluorescence anisotropies for $\beta=0°$ and $90°$ using equations (4), (15), (16) and (22) at time zero yields the first two ground state order parameters for rhodamine 6G. A least squares analysis (Microcal Origin) of the single photon $\beta=0°$ anisotropy decay yields the cylindrically symmetric alignment relaxation time τ_{20}, the corresponding $\beta=90°$ is fitted to equation (22) using the previously determined values for the ground state order parameters and the cylindrically symmetric alignment relaxation time τ_{20}. The two photon anisotropy analysis proceeds in a similar manner, however the first two ground state order parameters are known (to within experimental error), these are used in conjunction with the initial anisotropy measurements to obtain an initial value for $K'=6$. Analysis of the $\beta=0°$ anisotropy decay yields an independent value τ_{20}. Finally the $\beta=90°$ decay is analysed as above but with the three order parameters allowed to float within their error margins. The least squares fits produced in this manner are overlaid on the data in figure 5. The order parameters, alignment relaxation times and diffusion rates ($D_{\perp}^{LAB}$ and $D_{\parallel}^{LAB}$) determined from the data are displayed in table 1.

5.1 Molecular Order Parameters and the Orientational Distribution Function

In terms of the normalised moments $\left\langle \alpha_{KO}^{gs}(ss) \right\rangle$ the ground state distribution function is given by

$$P_{gs}(\theta,\phi) = \left\langle C_{00}^{gs}(ss) \right\rangle \left[Y_{00}(\theta,\phi) + \sum_{K\geq 2(even)} \left\langle \alpha_{K0}^{gs}(ss) \right\rangle Y_{K0}(\theta,\phi) \right] \tag{23}$$

Conservation of orientational probability requires $\left\langle C_{00}^{gs}(ss) \right\rangle = 1/\sqrt{4\pi}$ [7] and (23) can be written as

$$P_{gs}(\theta,\phi) = \frac{1}{4\pi} \left[Y_{00}(\theta,\phi) + \sqrt{4\pi} \sum_{K\geq 2(even)} \left\langle \alpha_{K0}^{gs}(ss) \right\rangle Y_{K0}(\theta,\phi) \right] \tag{24}$$

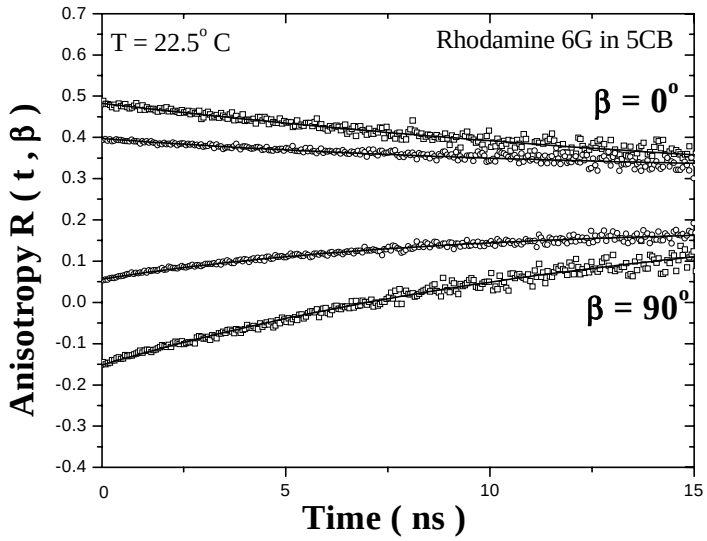

Figure 5. Anisotropy decays measured for rhodamine 6G in 5CB at 22.5°C. The upper and lower anisotropy decays are obtained with two photon excitation at β=0°and β=90°respectively. The solid lines are the result of the least squares fitting procedure described above.

	Single Photon	**Two Photon**
$\tau_{20}(\times 10^{-9}\text{s})$	10.615±1.5	10.7±0.2
$\tau_{22}(\times 10^{-9}\text{s})$	5.8±0.7	6.1±0.9
$D_{\perp}(\times 10^{7}\text{s}^{-1})$	1.57±0.23	1.56±0.03
$D_{\parallel}(\times 10^{7}\text{s}^{-1})$	3.54±0.44	3.350.61
$A = \frac{D_{\parallel}}{D_{\perp}} = \frac{\gamma_{\phi}}{\gamma_{\theta}}$	2.26±0.05	2.14±0.35
$\frac{\langle \alpha_{20}^{ex}(ss) \rangle}{\sqrt{5}}$	0.31±0.06	0.34±0.05
$\frac{\langle \alpha_{20}^{gs}(ss) \rangle}{\sqrt{5}} \equiv \langle P_2 \rangle$	0.24±0.06	0.30±.0.03
$\langle \alpha_{40}^{gs}(ss) \rangle \equiv 3\langle P_4 \rangle$	-0.55±0.07	-0.53±0.08
$\langle \alpha_{60}^{gs}(ss) \rangle \equiv \sqrt{13}\langle P_6 \rangle$	--	-0.51±0.09

Table 1 Orientational relaxation data and equilibrium order parameters obtained for rhodamine 6G in 5CB. The cylindrically symmetric and asymmetric alignment relaxation times (τ_{20} and τ_{22}) are used to determine the intrinsic θ and ϕ diffusion coefficients ($D_{\perp}$ and $D_{\parallel}$). The ground state order parameters were obtained from fits to the initial fluorescence anisotropies and the β=90° anisotropy signals (see above). The equilibrium excited state alignment values are determined from least squares fits to the anisotropy decays.

Substitution of the normalised moments from Table 1 into (24) yields the 'raw' distribution functions shown in Figure 6(a). Both distributions are peaked in the vicinity of 35°-45° (there is an equivalent peak at 180°-θ due to the even parity of the distribution function), but show regions of negative probability which is physically unreasonable and indicates that higher moments are necessarily present in (24). Determination of 'hidden' order parameters has been demonstrated by Durbin et al.[14]. Here varying values of higher moments are added sequentially but in decreasing magnitude to the raw distribution function in such a manner that the regions of negative probability are removed with the constraint that $P(\theta,\phi)$ retain a single maximum between 0 and 90°. Using this approach to both sets of data additional order parameters up to K=12 are found, their values together with those of the observed order parameters are shown in Table 2, the resulting probability distribution functions are plotted in Figure 6(b). Both distributions are closely approximated by Gaussian functions with maxima at c.a. 38° (and c.a. 142°) to the nematic director with a width of c.a. 26°. From table 1 it can be seen that to within experimental error the ground and excited state equilibrium degrees of alignment are equal, and it is reasonable in this light to assume that the ground and excited state environments for rhodamine 6G in 5CB are similar.

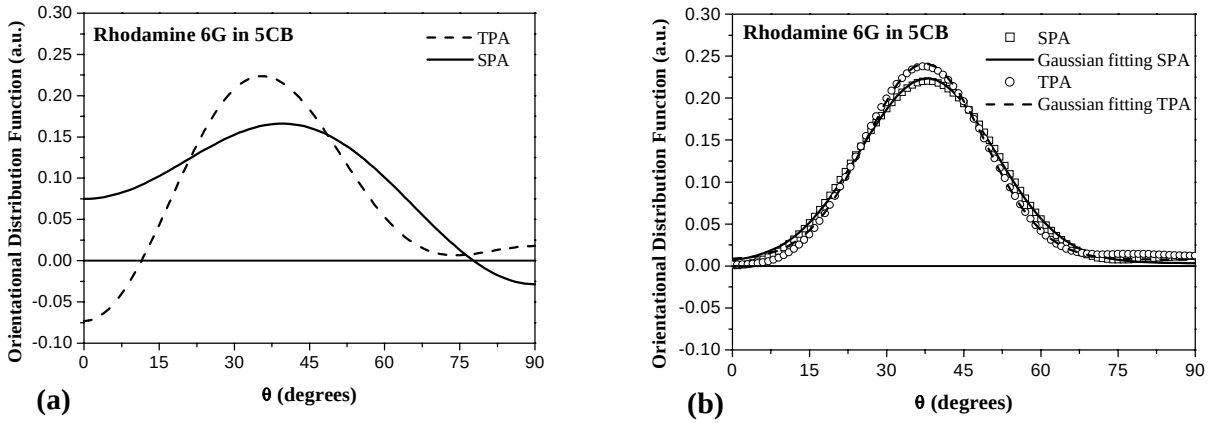

Figure 6: (a) Raw orientational distribution functions for rhodamine 6G in 5CB at 22.5°C, both single photon and two photon data indicate a preferential molecular orientation at 35°-45° to the nematic director, however both display regions of negative probability indicating that additional (higher) moments must be present. 7(b) Orientational distribution functions obtained by the addition of higher order parameters along the lines of Durbin et al.[14], both distributions are Gaussian with maxima at 37.9° (single photon data) and 37.5° (two photon results), the Gaussian widths are 26.3°and 23.1° respectively.-

	Single Photon	Two Photon
$\langle \alpha_{40}^{gs}(ss) \rangle \equiv \sqrt{5}\langle P_4 \rangle$	0.541	0.664
$\langle \alpha_{40}^{gs}(ss) \rangle \equiv 3\langle P_4 \rangle$	-0.545	-0.528
$\langle \alpha_{60}^{gs}(ss) \rangle \equiv \sqrt{13}\langle P_6 \rangle$	-0.461(*)	-0.513
$\langle \alpha_{80}^{gs}(ss) \rangle \equiv \sqrt{17}\langle P_8 \rangle$	0.096(*)	0.149(*)
$\langle \alpha_{100}^{gs}(ss) \rangle \equiv \sqrt{21}\langle P_{100} \rangle$	0.059(*)	0.056(*)
$\langle \alpha_{120}^{gs}(ss) \rangle \equiv 5\langle P_{120} \rangle$	-0.004(*)	-0.004(*)

Table 2 Measured and extrapolated (*) normalised order parameters used to construct the rhodamine 6G distribution functions plotted in Figure 6(b)

5.2 Orientational Dynamics

From Table 1 it is clear that there is a marked difference in the cylindrically symmetric and asymmetric alignment dynamics of rhodamine 6G in the nematic phase of 5CB. From the values of $D_{\parallel}$ and $D_{\perp}$ the rate of ϕ diffusion is over twice that for θ relaxation. In an isotropic medium $D_{\parallel}$ and $D_{\perp}$ are necessarily equal[7]. In the nematic 5CB the range of allowed orientations for rhodamine 6G with respect to the director is significantly constrained (see figure 6(b)) whilst motion in the ϕ co-ordinate is unrestricted (all equilibrium values of moments with $Q \neq 0$ vanish in the nematic phase). Both single and two photon measurements yield similar values for τ_{20} and τ_{22}. The increased angular precision in two photon excitation results in a greater displacement of the initial cylindrically symmetric molecular alignment from equilibrium allowing for a more accurate determination of the slower τ_{20} relaxation time (reduced uncertainty) over the finite data collection range imposed by signal to noise considerations.

6. CONCLUSIONS

We have shown that single and two photon photoselection techniques in conjunction with time resolved polarised fluorescence measurements can provide detailed information on the motion and order of a molecular probe in an anisotropic medium. Measurement of the intrinsic θ and ϕ diffusion rates for rhodamine 6G together with the equilibrium order parameters show that the order imposed by the nematic host is accompanied by highly restricted rotational diffusion.

7. REFERENCES

1. G. R. Fleming, "*Chemical Applications of Ultrafast Spectroscopy*", Claredon Press, Oxford (1986).
2. J. R Lakowicz ,"*Principles of Fluorescence Spectroscopy*", Plenum, New York, (1999).
3. A. J. Bain. "*Time Resolved Polarised Fluorescence Studies of Ordered Molecular Systems*", in An Introduction to Laser Spectroscopy, Eds D. L. Andrews and A. Demidov (Kluwer 2002).
4. J. Kinoshita, S. Kawato and A. Ikegami, Biophys. J., **20**, 289, (1997)
5. N. Chadborn, J. Bryant, A. J. Bain and P. O'Shea, Biophys J., **76**, 2198, (1999)
6. A. J. Bain, P. Chandna and G. Butcher, Chem Phys Lett, **260**, 441 (1996)
7. A. J. Bain, P. Chandna ,and J. Bryant, J. Chem. Phys , **112**, 10418, (2000)
8. A. J. Bain, P. Chandna, G. Butcher and J. Bryant, J. Chem. Phys , **112**, 10435, (2000)
9. A. J. Bain and J. Bryant, Proc. of CLEO/QELS. Paper QThC5, (1999)
10. E. M. Monge, D. Armoogun, J. Bryant and A. J. Bain, to be published
11. E. M. Monge, A. Harsono, J. Bryant, B. Obradovic and A. J. Bain, Proc. Of British Liquid Crystal Society Annual Meeting 2002 (unpublished)
12. D. Armoogum, E. M. Monge and A. J. Bain, Proc. SPIE's 47th Annual Meeting 2002, Vol **4799** Paper 17
13. S. Jen, N. A. Clark, P.S. Pershan and E. B. Priestley, J. Chem. Phys. **66**, 4635 (1977)
14. Durbin S. D and Shen Y. R, Phys. Rev. A, **30(3)**, 1419 (1984)
15. S. Chandraesekhar, "*Liquid Crystals*" 2nd Ed. Cambridge University Press, 1992
16. A. J. Bain and A. J. McCaffery, J. Chem Phys., **80**, 5893 (1984)
17. A. J. Bain and A. J. McCaffery, J. Chem Phys., **83**, 2632 (1985)
18. A. J. Bain and A. J. McCaffery, J. Chem Phys., **83**, 2641 (1985)
19. D. M Brink and G. R Satchler, "*Angular Momentum*", 3rd addition, Oxford Science (1993)
20. D. A. Varshalovich, A. N. Moskalev and V. K. Khersonskii, "*Quantum Theory of Angular Momentum*", Ed World Scientific, London (1989)
21. S. T. Wu, C. S. Wu, M. Warenghem and M. Ismaili, Opt. Eng, **32 (8)**, 1775 (1993)
22. J. Bryant Ph.D. thesis, University of Essex (2000)